

Enhanced Twist-Averaging Technique for Magnetic Metals: Applications using Quantum Monte Carlo

Gani Annaberdiyev

P. Ganesh and J. T. Krogel

Oak Ridge National Laboratory, Oak Ridge, Tennessee 37831, USA
Email: annaberdiyea@ornl.gov

QMCPACK Workshop
December 14, 2023 | Argonne National Laboratory, Lemont, IL

ORNL is managed by UT-Battelle LLC for the US Department of Energy



Introduction

- In quantum Monte Carlo (QMC), twist-averaging (TA) is unavoidable in metallic systems to achieve practical results.
- Yet, the question of how the chosen set of \mathbf{k} -points should be occupied in metallic systems persists without a definitive, standardized approach.
- We propose an improved grand-canonical TA (GCTA) scheme, which aims to reproduce the reference magnetization and achieves charge neutrality by construction.
- Thus it avoids the large energy fluctuations and the postprocessing needed to correct the energies.
- It shows the most robust convergence of total energy and magnetism to the thermodynamic limit (TDL) when compared against four other TA schemes.
- Diffusion Monte Carlo applications are shown on Al (fcc) and alpha-Fe (bcc).
- Overall, smooth convergence is observed for total, kinetic, and potential energies, cell magnetization, atomic moments, and charge densities.

Theory And Methodology: Twist-Averaging Methods (Part I)

$$\begin{aligned}\Psi_{\mathbf{k}_s}(\mathbf{r}_1, \dots, \mathbf{r}_n + \mathbf{R}_s, \dots, \mathbf{r}_{N_e^s}) &= \\ &= \exp(i\mathbf{k}_s \cdot \mathbf{R}_s) \Psi_{\mathbf{k}_s}(\mathbf{r}_1, \dots, \mathbf{r}_n, \dots, \mathbf{r}_{N_e^s})\end{aligned}$$

$$\langle \hat{O} \rangle = \frac{1}{Z_\theta} \left\langle \Psi_{\mathbf{k}_s} \left| \hat{O} \right| \Psi_{\mathbf{k}_s} \right\rangle$$

CTA-DFT: Canonical twist-averaging (CTA) using the lowest DFT eigenvalues. Each twist is charge neutral, but exhibits a fluctuating magnetic moment, if present.

CTA-INS: Canonical twist-averaging used in insulators. Each twist is charge neutral and exhibits no fluctuating magnetic moment.

CTA fails to accurately represent the discontinuity of occupations at the Fermi level!

GCTA-DFT: Conventional GCTA that occupies single-particle levels in each super twist strictly based on the Fermi level obtained using DFT in TDL (dense \mathbf{k} -mesh).

$$N_{\uparrow/\downarrow}^s(\theta) = \sum_i^{N_{\text{KS}}^p} f_{\uparrow/\downarrow}(i)$$

$$f_{\uparrow/\downarrow}(i) = \begin{cases} 1, & \text{if } (\varepsilon_i^{\uparrow/\downarrow} < E_F) \\ 0, & \text{otherwise.} \end{cases}$$

$$E_F = E_F^{\text{DFT}}$$

$$Q_{\text{TA}} = \sum_\theta \frac{q(\theta)}{Z_\theta} \neq 0.$$

GCTA-DFT net charge is nonzero. This means wildly fluctuating energies and charge densities!

Theory And Methodology: Twist-Averaging Methods (Part II)

GCTA-AFL: GCTA with adapted Fermi level. In this improved scheme, the orbital occupations are similar to the conventional GCTA, but the Fermi level is shifted so that the twist-averaged system is charge neutral for any value of Z_θ . Consider a set which contains the sorted list of all KS eigenvalues of a supercell characterized by Z_T and Z_θ :

$$\mathcal{E}_i = \{\varepsilon_1^\chi, \varepsilon_2^\chi, \dots, \varepsilon_i^\chi, \dots, \varepsilon_L^\chi\} \quad (\forall i \quad \varepsilon_i^\chi < \varepsilon_{i+1}^\chi)$$

$$\chi = \{\uparrow, \downarrow\} \qquad L = 2 \cdot N_{\text{KS}}^{\text{p}} \cdot Z_T \cdot Z_\theta$$

$$\lambda = N_e^{\text{p}} \cdot Z_T \cdot Z_\theta$$

$$E_F^{\text{AFL}} = \frac{\mathcal{E}_\lambda + \mathcal{E}_{\lambda+1}}{2}$$

The result is $Q_{\text{TA}} = 0$ by definition, at the price of a fluctuating E_F as Z_T or Z_θ is changed. In addition, E_F is set globally for both spin channels, which can introduce a small deviation to the reference magnetization.

GCTA-SAFL: GCTA with spin-adapted Fermi level. Here, the Fermi levels for up and down channels are shifted independently to target the reference cell magnetization, which is the DFT magnetization throughout this work. The KS eigenvalues are now sorted separately for each spin channel:

$$\mathcal{E}_i^\uparrow = \left\{ \varepsilon_1^\uparrow, \varepsilon_2^\uparrow, \dots, \varepsilon_i^\uparrow, \dots, \varepsilon_\ell^\uparrow \right\} \quad (\forall i \quad \varepsilon_i^\uparrow < \varepsilon_{i+1}^\uparrow)$$

$$\mathcal{E}_i^\downarrow = \left\{ \varepsilon_1^\downarrow, \varepsilon_2^\downarrow, \dots, \varepsilon_i^\downarrow, \dots, \varepsilon_\ell^\downarrow \right\} \quad (\forall i \quad \varepsilon_i^\downarrow < \varepsilon_{i+1}^\downarrow)$$

$$u = \text{Round} \left[\frac{(N_e^{\text{p}} + M_{\text{DFT}}^{\text{p}}) \cdot Z_T \cdot Z_\theta}{2} \right]$$

$$d = (N_e^{\text{p}} \cdot Z_T \cdot Z_\theta) - u$$

$$E_F^{\text{SAFL-}\uparrow} = \frac{\mathcal{E}_u^\uparrow + \mathcal{E}_{u+1}^\uparrow}{2} \qquad E_F^{\text{SAFL-}\downarrow} = \frac{\mathcal{E}_d^\downarrow + \mathcal{E}_{d+1}^\downarrow}{2}$$

This again results in $Q_{\text{TA}} = 0$ but also closely follows the reference magnetization.

Results: Twist-Mesh Size Convergence (Al, Part I)

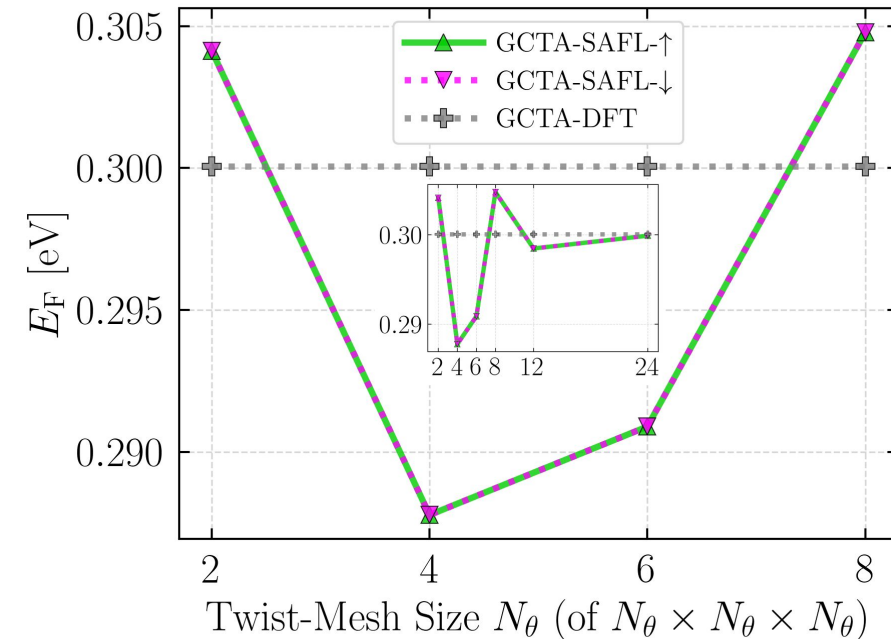
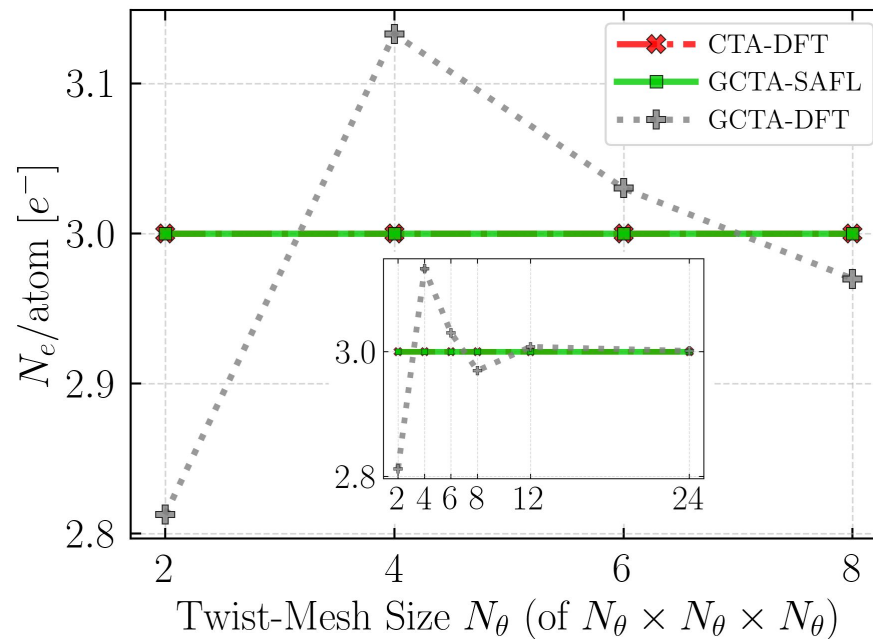


FIG. 1: Convergence of various twist-averaged quantities of fcc Al (4 Al atoms) with respect to the employed QMC twist-mesh. (left) Number of electrons in QMC, (right) Fermi levels set in QMC. The twist-mesh is uniform in the reciprocal space and includes the high-symmetry points [Γ , X, M, R]. QMC errors are one standard deviation and smaller than the data symbol sizes.

Results: Twist-Mesh Size Convergence (Al, Part II)

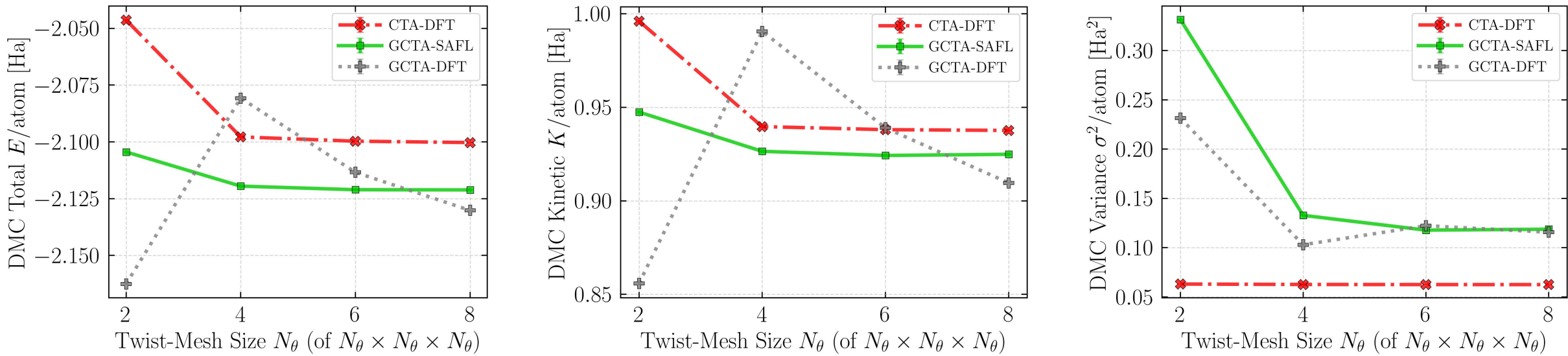


FIG. 2: Convergence of various twist-averaged quantities of fcc Al (4 Al atoms) with respect to the employed QMC twist-mesh. (left) DMC total energy, (middle) DMC kinetic energy, (right) DMC total energy variance. The twist-mesh is uniform in the reciprocal space and includes the high-symmetry points [Γ , X, M, R]. QMC errors are one standard deviation and smaller than the data symbol sizes.

Results: Twist-Mesh Size Convergence (Fe, Part I)

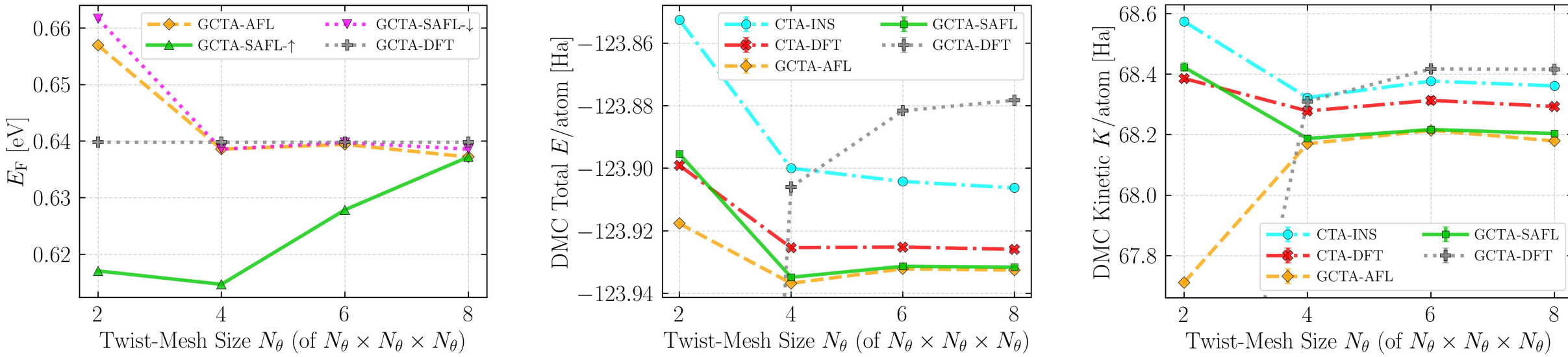


FIG. 3: Convergence of various twist-averaged quantities of bcc Fe (2 Fe atoms) with respect to the employed QMC twist-mesh. (left) Fermi levels set in QMC, (middle) DMC total energy, (right) DMC kinetic energy. The twist-mesh is uniform in the reciprocal space and includes the high-symmetry points [Γ , X, M, R]. QMC errors are one standard deviation and smaller than the data symbol sizes.

Results: Twist-Mesh Size Convergence (Fe, Part II)

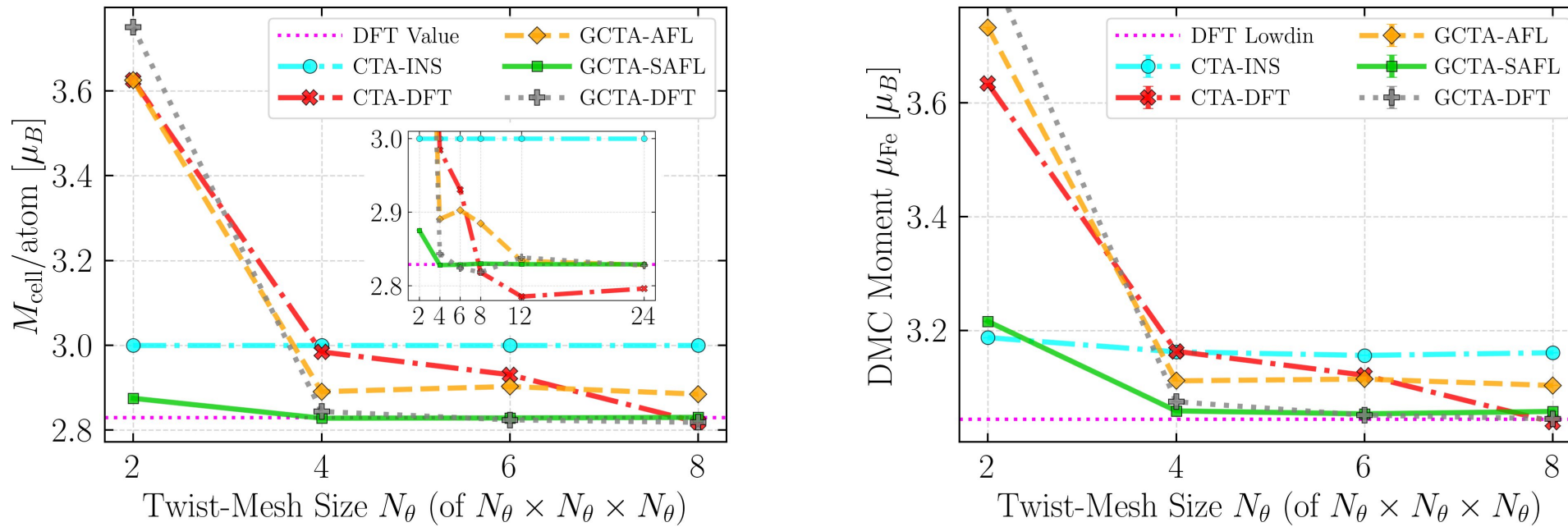


FIG. 4: Convergence of various twist-averaged quantities of bcc Fe (2 Fe atoms) with respect to the employed QMC twist-mesh. (left) Cell magnetization, (right) DMC atomic moment. The twist-mesh is uniform in the reciprocal space and includes the high-symmetry points $[\Gamma, X, M, R]$. QMC errors are one standard deviation and smaller than the data symbol sizes.

Results: Supercell Size Convergence (Al)

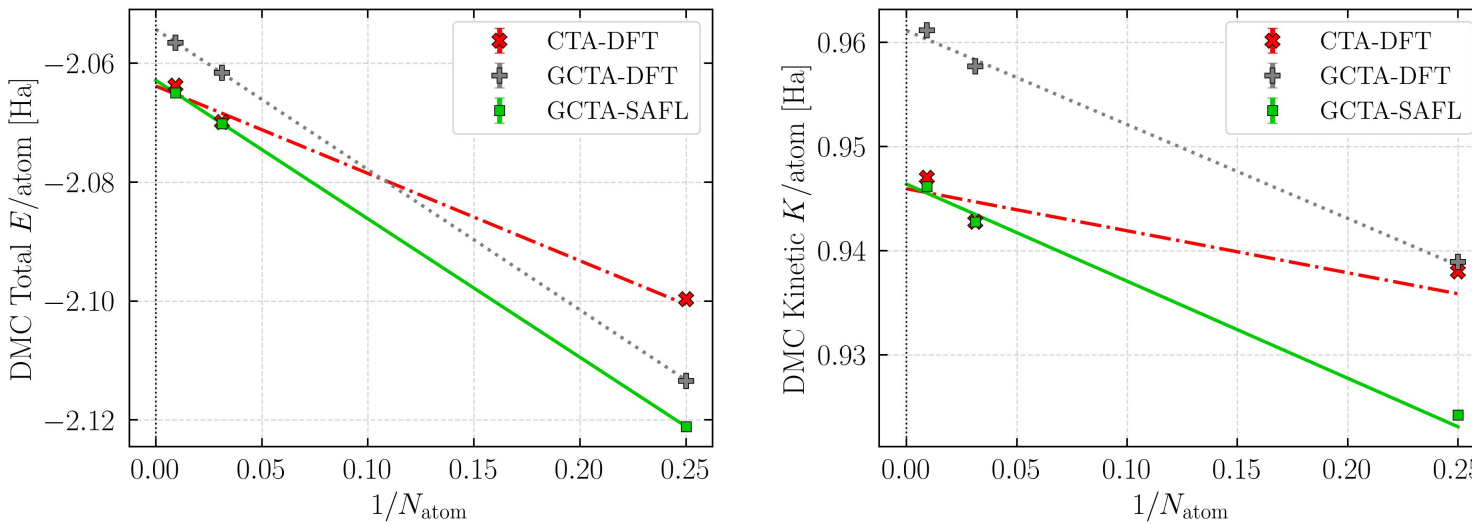


FIG. 5: TDL convergence of twist-averaged DMC energies of fcc Al as the supercell is expanded. (left) DMC total energy, (right) DMC kinetic energy. $Z_T \cdot Z_\theta = 6^3$ is kept constant as the supercell is increased. QMC errors are one standard deviation and smaller than the data symbol sizes.

TABLE : Cohesive energies [eV] of Al predicted by various methods. The theoretical values do not include the zero-point-energy (ZPE) contributions. The experimentally reported number (327.320 ± 4.2 kJ/mol) was corrected for ZPE (0.04 eV) [64] for consistency with the theory.

Method	E_{coh} [eV]	Ref.
LDA	3.884	this work
HF	1.388	[60]
CCSD	2.966	[60]
CCSD(T) _{SR}	3.102	[60]
CCSD-SVC	3.347	[60]
DMC/SJ	3.341(1)	[25]
DMC/BF	3.403(1)	[25]
DMC/SJ	3.438(27)	this work
Experiment	3.432(44)	[65]

$$E_{\text{coh}}^{\text{Al}} = 3.438 \pm 0.026_{\text{(syst)}} \pm 0.002_{\text{(stat)}} \text{ eV}$$

[this work] To be submitted to arXiv.

[25] Hood, R. Q., Kent, P. R. C. & Reboredo, F. A. Diffusion quantum Monte Carlo study of the equation of state and point defects in aluminum. *Phys. Rev. B* 85, 134109 (2012).

[60] Neufeld, V. A., Ye, H.-Z. & Berkelbach, T. C. Ground-State Properties of Metallic Solids from Ab Initio Coupled-Cluster Theory. *J. Phys. Chem. Lett.* 13, 7497–7503 (2022).

[64] Zhang, G.-X., Reilly, A. M., Tkatchenko, A. & Scheffler, M. Performance of various density-functional approximations for cohesive properties of 64 bulk solids. *New J. Phys.* 20, 063020 (2018).

[65] Chase, Jr., M. W. et al. JANAF Thermochemical Tables. *J. Phys. Chem. Ref. Data* 14, 65 (1985).

Results: Supercell Size Convergence (Fe)

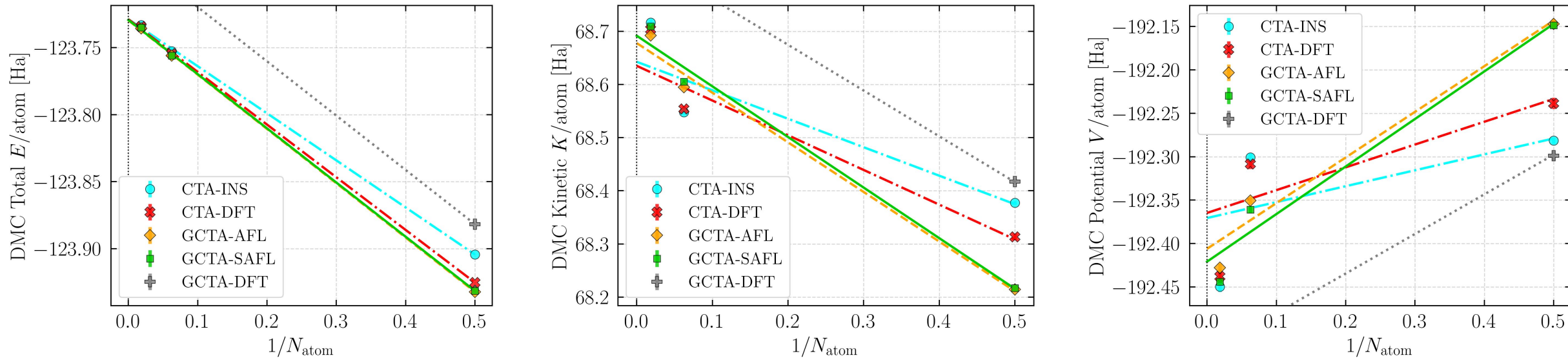


FIG. 6: TDL convergence of twist-averaged DMC energies of alpha-Fe as the supercell is expanded. (left) DMC total energy, (middle) DMC kinetic energy, (right) DMC potential energy. $Z_T \cdot Z_\theta = 6^3$ is kept constant as the supercell is increased. QMC errors are one standard deviation and smaller than the data symbol sizes in most cases.

Discussion

- GCTA-(S)AFL use cases: metal-insulator-transition, equation-of-state for lattice parameters, Fermi surface.
- Here we employed a uniform grid. But GCTA-(S)AFL does not require this and any type of k -point set can be used (pseudo-random, quasi-random).
- GCTA-SAFL is only applicable in collinear systems. For non-collinear, use GCTA-AFL and keep the ($Z_T \cdot Z_\theta = \text{Constant}$) to maintain the same state, or use large ($Z_T \cdot Z_\theta$) value to converge the magnetization.
- GCTA-(S)AFL will be implemented on Nexus in the future. Currently, it's user's responsibility to set the correct twist-number, and up/down occupations in each twist input:

```
<particleset name="e" random="yes" randomsrc="ion0">
  <group name="u" size="19" mass="1.0">
    <parameter name="charge"          > -1      </parameter>
    <parameter name="mass"           > 1.0      </parameter>
  </group>
  <group name="d" size="14" mass="1.0">
    <parameter name="charge"          > -1      </parameter>
    <parameter name="mass"           > 1.0      </parameter>
  </group>
</particleset>
```

```
<sposet_builder type="bspline" href="../nscf/pwscf_output/pwscf.pwscf.h5"
  tilematrix="1 0 0 0 1 0 0 0 1" twistnum="0" source="ion0" version="0.10"
  meshfactor="1.0" precision="float" truncate="no">
  <sposet type="bspline" name="spo_u" size="19" spindataset="0"/>
  <sposet type="bspline" name="spo_d" size="14" spindataset="1"/>
</sposet_builder>

<determinantset>
  <slaterdeterminant>
    <determinant id="updet" group="u" sposet="spo_u" size="19"/>
    <determinant id="downdet" group="d" sposet="spo_d" size="14"/>
  </slaterdeterminant>
</determinantset>
```

FIG. 7: Sections requiring changes (red rectangles) in the QMCPACK input to obtain GCTA-(S)AFL occupations.

Conclusions

- We proposed GCTA-(S)AFL as an improved version of the conventionally used GCTA-DFT.
- **GCTA-SAFL** shows the overall best convergence to TDL in the context of total energies and magnetism.
- **GCTA-SAFL** shows a rapid convergence of energy components and magnetic moments as number of twist is increased for a given simulation cell.
- GCTA-(S)AFL result in lower total energies than CTA-DFT for large number of twists.
- GCTA-(S)AFL exhibit robust supercell extrapolations, allowing the use of only the smallest cells.
- The proposed change is simple and only requires the availability of the single-particle orbital eigenvalues for each twist and light pre-processing to set the up/down occupations in the QMC input.
- These schemes **do not require any post-processing** corrections.

Thank you! Questions?



P. Ganesh



J. T. Krogel

Results: Supercell Size Convergence (Fe, Part II)

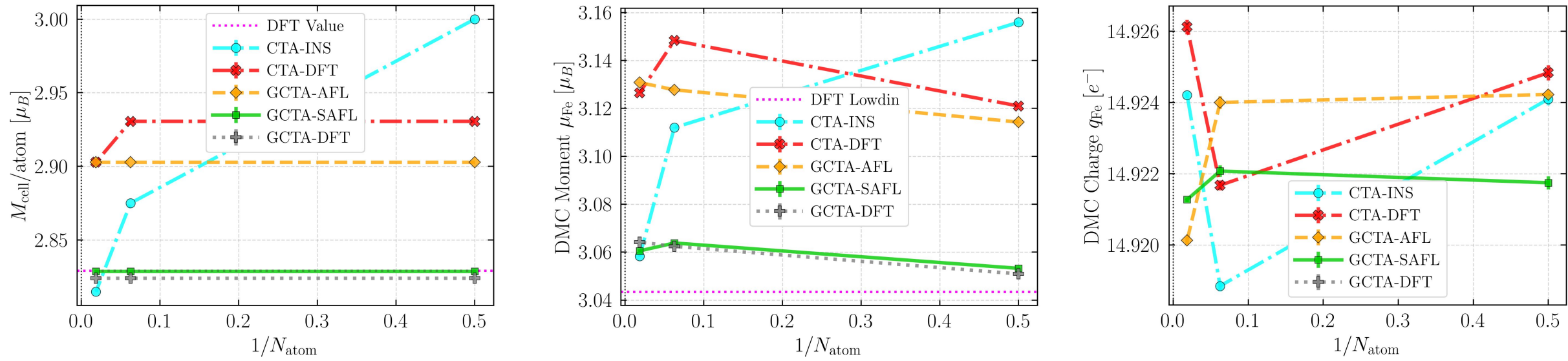


FIG: TDL convergence of twist-averaged DMC quantities of alpha-Fe as the supercell is expanded. (left) Cell magnetization, (middle) DMC atomic moment, (right) DMC atomic charge. $Z_T \cdot Z_\theta = 6^3$ is kept constant as the supercell is increased. QMC errors are one standard deviation and smaller than the data symbol sizes in most cases.

Theory And Methodology: Computational Details

- We used experimental geometries extrapolated to $T = 0$ K temperature for both Al (fcc) and alpha-Fe (bcc).
- Γ -centered mesh with an even grid ($Z_\theta = N_\theta^3$ where $N_\theta \in \text{even}$) was used to consistently include high-symmetry points.
- Use the fcc (4 Al atoms) and bcc (2 Fe atoms) conventional cells to tile the [2×2×2] and [3×3×3] supercells.
- Correlation consistent effective core potentials were used (ccECP for Al and ccECP-soft for Fe).
- The KS orbitals were converged at [24×24×24] \mathbf{k} -mesh in the BZ using 400 Ry kinetic energy cutoff.
- DFT XC functionals: LDA for Al and LDA+U(5.5 eV) for alpha-Fe.
- DMC calculations: Slater-Jastrow, standard Ewald, $\Delta\tau = 0.005 \text{ Ha}^{-1}$, size-consistent T-moves.
- Up/down charge densities were accumulated as a grid histogram with [100×100×100] points / conv. cell.
- Extrapolated DMC moments and charges using spherical integration radius (R_c = nearest-neighbor midpoint).
- All Jastrow factors were optimized for energy at $\mathbf{k} = \Gamma$ twist and reused at other twists.
- Importantly, **no post-processing** to correct the energies. Only raw quantities are reported.